行政院國家科學委員會專題研究計畫　期中進度報告

量子流體力學-理論與計算(1/2)

計畫類別： 個別型計畫
計畫編號： NSC93-2212-E-002-040-
執行期間： 93 年 08 月 01 日至 94 年 07 月 31 日
執行單位： 國立臺灣大學應用力學研究所

計畫主持人： 楊照彥

計畫參與人員： 楊照彥　黃俊誠　謝澤揚

報告類型： 精簡報告
報告附件： 出席國際會議研究心得報告及發表論文
處理方式： 本計畫可公開查詢

中　華　民　國 94 年 5 月 31 日

量子流體力學-理論與計算(1/2) 進度報告

楊照彥

國立臺灣大學應用力學研究所

摘要

近來量子流體力學的研究在各個領域蓬勃發展，在 de Broglie-Bohm 方法中將複數的波函數以極座標形式來表達，再將其代入非線性薛丁格方程式之中，就可以得到一組相對應的量子流體力學方程式，其中有類比於古典流體力學的密度、速度，但亦有新的量子位能與壓力項出現，它們將是產生量子行為的因素，量子位能有著特殊的形式，它與密度之量值和變化量相關，量子流體力學形式裡當波函數為零時，即會造成有奇異的現象發生，此即是在超流體中漩渦的現象，奇異的現象在數值計算上亦會造成若干的困難，故建立一套解量子流體力學的數值方法除要考量其精確性外，對於奇異問題的處理更是一大重點。

本計畫目前所進行之工作主要分成兩個方向，一為利用高解析流體守恆律算則來解量子流體力學方程式，利用量子流體力學方程式與古典流體力學方程式相似的特性，便可將計算流體力學的方法運用在計算量子力學的問題之中，二為利用高精確度的徑向基底函數展開法來解非線性薛丁格方程式與量子流體力學方程式，徑向基底函數展開法是一種無網格且高精確的方法，所以運用在計算當中非常地有效率。 從現階段的結果中可以發現到各種流體的現象，並且可以發現一些量子流體特有之性質。

Abstract

Recently, interest in the de Broglie-Bohm formulation of quantum mechanics has increased dramatically within various fields. In the de Broglie-Bohm approach, the complex wave function is expressed in polar form and substituted into the time-dependent linear or nonlinear Schrödinger equation results a set of hydrodynamic-like equations which describe the flow of the probability. This set of equations are very similar to those of classical hydrodynamics except that an additional quantum potential term is present. The quantum potential and its associated quantum force give rise to all quantum effects such as tunneling and interference. Despite its conceptually attractive features, there are major computational problems inherent to the de Broglie-Bohm approach when a direct numerical solution of the quantum hydrodynamics is attempted. In particular, the quantum potential possess some unique features, it does not respond to the intensity of the wave but rather depends upon its form. A desirable numerical method for solving the quantum hydrodynamics based on Schrödinger equation not only requires high accuracy but also the ability to handle discontinuities caused by the singularity of quantum potential. The current work has two independent directions: one is high resolution scheme, the other is radial basis function based scheme.

Nonlinear Schrödinger Equation

The dynamics of N identical pairwise interacting quantum particles is governed by the time-dependent, N-body Schrödinger equation

$$i\hbar\frac{\partial\Psi}{\partial t}=-\frac{\hbar^2}{2m}\Delta^N\Psi+\sum_{\substack{i,j=1\\ i\neq j}}^{N}W\left(\vec{x}_i-\vec{x}_j\right)\Psi+\sum_{i=1}^{N}V\left(\vec{x}_i\right)\Psi \qquad (1)$$

where $\vec{x}_i=\left(x_{i1},x_{i2},x_{i3}\right)$, $\Psi\left(\vec{x}_1,\vec{x}_2,\vec{x}_3,\cdots,\vec{x}_N,t\right)$ is the wave function of the N-particle system, $\Delta^N=\left(\nabla^N\right)^2=\sum_{i=1}^{N}\left(\partial_{x_{i1}}^2+\partial_{x_{i2}}^2+\partial_{x_{i3}}^2\right)$ is the kinetic energy or Laplacian operator for N particles, $W\left(\vec{x}_i-\vec{x}_j\right)$ is the symmetric interaction potential between the *i*th and *j*th particle. Also, ħ is Plank's constant divided by 2π and m is the mass of the particles under consideration. One way to arrive at a mean-field description is by using the Lagrangian reduction technique, which exploits the Hamiltonian structure of (1). The Lagrangian of (1) is given by

$$L=\int_{-\infty}^{\infty}\left\{i\frac{\hbar}{2}\left(\Psi\frac{\partial\Psi^*}{\partial t}-\Psi^*\frac{\partial\Psi}{\partial t}\right)+\frac{\hbar^2}{2m}\left|\nabla^N\Psi\right|^2+\sum_{i=1}^{N}\left(\sum_{j\neq i}^{N}W\left(\vec{x}_i-\vec{x}_j\right)+V\left(\vec{x}_i\right)\right)\left|\Psi\right|^2\right\}d\vec{x}_1d\vec{x}_2\cdots d\vec{x}_N \qquad (2)$$

Using Hartree-Fock approximation and identical particle assumption results in the Euler-Lagrange equation

$$i\hbar\frac{\partial\psi\left(\vec{x},t\right)}{\partial t}=-\frac{\hbar^2}{2m}\Delta\psi\left(\vec{x},t\right)+V\left(\vec{x}\right)\psi\left(\vec{x},t\right)+\left(N-1\right)\psi\left(\vec{x},t\right)\int_{-\infty}^{\infty}W\left(\vec{x}-\vec{y}\right)\left|\psi\left(\vec{y},t\right)\right|^2d\vec{y} \qquad (3)$$

Here, $\vec{x}=\vec{x}_i$, and Δ is the one-particle Laplacian in three dimensions. The

Euler-Lagrange equation (3) is identical for all $\psi(\vec{x}_i,t)$. (3) describe the non-linear, non-local, mean-field dynamics of the wave function $\psi(\vec{x},t)$. The last term in (3) represents the effective potential acting on $\psi(\vec{x},t)$ due to the presence of the other particles. At this point, it is common to make an assumption on the functional form of the interaction potential $W(\vec{x}-\vec{y})$. One convenient assumption in the case of short-range potential interaction is $W(\vec{x}-\vec{y})=\kappa\delta(\vec{x}-\vec{y})$ where δ is the Dirac delta function. This leads to the Gross-Pitaevskii mean-field description:

$$i\hbar\frac{\partial\psi}{\partial t}=-\frac{\hbar^2}{2m}\Delta\psi+\beta|\psi|^2\psi+V(\vec{x})\psi \qquad (4)$$

where $\beta=(N-1)\kappa$ reflects whether the interaction is repulsive or attractive. The above string of assumption is difficult to physically justify. In the dilute-gas limit, (3) and (4) are asymptotically equivalent.

Quantum Fluid Dynamical Equations

Starting with the Gross-Pitaevskii equation (4) for a dilute gas, we write the wavefunction $\psi(\vec{x},t)=\sqrt{\rho(\vec{x},t)}\exp\{iS(\vec{x},t)/\hbar\}$ in terms of the phase and amplitude. This transformation is usually called Madelung's transformation and was originally introduced in the context of the linear Schrödinger equation for quantum mechanics. After substitution in (4) and separation of the real and imaginary parts of the equation, one obtains Quantum Fluid Dynamical Equations

$$\begin{aligned}&\frac{\partial\rho}{\partial t}+\nabla\cdot(\rho\nabla S/m)=0\\&\frac{\partial S}{\partial t}+\frac{1}{2m}|\nabla S|^2+\alpha\rho+V-\frac{\hbar^2}{2\sqrt{\rho}}\Delta\sqrt{\rho}=0\end{aligned} \qquad (5)$$

Looking at ρ as a density and φ as an hydrodynamic potential. The last term at right hand side of (5) corresponds to a "quantum potential" .

Define velocity $\vec{v}=\nabla S/m$,the QFD equations can be written in conservation law form with source terms.

$$\frac{\partial Q}{\partial t}+\frac{\partial F}{\partial x}=S \qquad Q=(\rho,\rho u)^T \qquad (6)$$

$$F=(\rho u,\rho u^2+p)^T \qquad S=\left(0,\rho\partial\left(V+V_q\right)/\partial x\right)$$

$$V_q=\frac{\hbar^2}{2m}\nabla^2\sqrt{\rho}/\sqrt{\rho} \qquad p(\rho)=g\rho^2/2m$$

Madelung's transformation is, however, singular when ψ vanishes. Since this field is complex, these "topological defects" are generically located on points in two space dimensions and on lines in three dimensions. In the context of superfluidity, they are known as "quantum vortices". The circulation of the velocity $\vec{v}=\nabla S/m$ around each of them is ±2π.

At the heart of the ρ-based QFD formulation is the assumption that the density ρ and phase S are more slowly varying functions than the generally oscillatory real and imaginary parts of the corresponding complex-valued wavefunction. The discussion above further suggests that the density ρ can be replaced by ln ρ without altering the nature of the QFD equations. This replacement has several suggestive numerical advantages. First ln ρ should be a more slowly varying function than its argument ρ, and working with the former should make the QFD method numerically even more expedient. Second, the practical dynamical range of ln ρ should be much smaller than that of ρ. Third the structure of ln ρ is in general simpler than that of ρ itself. So, with the wavefunction written as $\psi(\vec{x},t)=\exp\{(R+iS)/\hbar\}$ and following the same procedure leading to an equivalent QFD formulation:

$$\begin{aligned}&\frac{\partial S}{\partial t}+\frac{(\nabla S)^2}{2m}+V+Q+\beta\exp(\frac{2R}{\hbar})=0\\&\frac{\partial R}{\partial t}+\frac{1}{m}\left\{\nabla R\cdot\nabla S+\frac{\hbar}{2}\nabla^2 S\right\}=0\end{aligned} \qquad (7)$$

where $Q=-\{(\nabla R)^2+\hbar\nabla^2 R\}/2m$ is the quantum potential.

Numerical Scheme

(i) High resolution scheme

Here, we adopt the method presented in [14] to solve the quantum fluid dynamics equations. Other class of methods such as weighted ENO methods [12,16] can also be employed. The Eq. (6) is discretized and expressed in the form of a conservative scheme:

$$\begin{aligned}&Q_j^{n+1}=Q_j^n-\lambda\left(F_{j+1/2}^n-F_{j-1/2}^n\right),\\&F_{j+1/2}^n=\frac{1}{2}\left(F_j^n+F_{j+1}^n+R_{j+1/2}\Phi_{j+1/2}\right)\end{aligned} \qquad (8)$$

Here $\phi_{j+1/2}^l$ are the elements of vector $\Phi_{j+1/2}$ and are defined by:

$$\begin{aligned}\phi_{j+1/2}^l=&\sigma\left(\alpha_{j+1/2}^l\right)\left(g_j^l+g_{j+1}^l\right)+\\&\xi\bar{\sigma}\left(\alpha_{j+1/2}^l\right)\left(d_j^l+d_{j+1}^l\right)-\varphi\left(\alpha_{j+1/2}^l+\gamma_{j+1/2}^l+\xi\delta_{j+1/2}^l\right)\end{aligned} \qquad (9)$$

where $\alpha_{j+1/2}^l=R_{j+1/2}^{-1}\left(Q_{j+1}-Q_j\right)$ is the characteristic variable difference, see [14] for details.

(ii) RBF scheme

We apply RBF in a method-of-lines (MOL) type approach for solving QFD equations. Consider an arbitrary set of N distinct scattered points $\vec{x}_1,\vec{x}_2,\cdots,\vec{x}_N$ and the corresponding

scattered data $f(\vec{x}_1), f(\vec{x}_2), \cdots, f(\vec{x}_N)$. The radial basis function interpolation can approximate the data points as function of space in the form

$$f(\vec{x}) = \sum_{i=1}^{N} \alpha_i \phi(\|\vec{x} - \vec{x}_i\|) = \sum_{i=1}^{N} \alpha_i \phi_i(\vec{x}) \qquad (10)$$

where ϕ_i is basis function centered at x_i and the real coefficients $\alpha_1, \alpha_2, \ldots, \alpha_N$ can be solved from the linear system:

$$y_j = \sum_{i=1}^{N} c_i \phi(\|\vec{x}_j - \vec{x}_i\|) = \sum_{i=1}^{N} c_i \phi_i(\vec{x}_j), \quad j = 1 \cdots N \qquad (11)$$

The gradient and Laplacian are taken by directly applying them to the interpolated function (9).

$$\nabla f(\vec{x}) = \sum_{i=1}^{N} \alpha_i \nabla \phi_i(\vec{x}) \qquad \nabla^2 f(\vec{x}) = \sum_{i=1}^{N} \alpha_i \nabla^2 \phi_i(\vec{x}) \qquad (12)$$

Multiquadrics are employed for spatially approximating the independent variables.

$$\phi_i(\vec{x}) = \sqrt{(\vec{x} - \vec{x}_i)^2 + c_i^2} \qquad (13)$$

where c_i are called shape parameters whose magnitudes are a key factor for obtaining accurate solutions. The time integration is done using a 4-th order Runge-Kutta method.

Numerical Experiments

(i) High resolution scheme

Some numerical experiments are tested to illustrate the method. The first example is a model for quasi-1D confinement in a standing light wave [13]. We use a sinusoidal potential $V(x) = -V_0 \sin^2(x)$ where V(x) = 0.5. In this case,V (x) is exactly a standing light wave. The initial conditions are

$$\rho(x,0) = V_0 \sin^2(x) + B, \qquad u(x,0) = \pm\sqrt{1 + \frac{V_0}{B}} \Big/ 1 + \frac{V_0}{B} \sin^2(x)$$

where the parameter B is set as 1.0. The exact solutions are same as the initial values. This example was computed using 401 grid points, with computational domain: $-4\pi \le x \le 4\pi$, and periodic boundary condtions were employed at both ends. The results were output after 12000 iterations at time 30. We compare the results of 1st order Roe's scheme (Roe1), 2nd order ENO scheme (ENO2) and WENO scheme with the exact solutions. The results are shown in Figure 1 and 2. It is noted that long time integration is possible with the present characteristics-based high resolution method and the higher order accuracy of results can be obtained. We also note that the treatment of source term due to quantum potential is crucial to the success of computation.

The second testing case we considered was the one presented in [17]. We used atomic units, and atomic mass m = 1a.u., g = 1/2, and let potential V (x) = 0. The exact solutions are given by

$$\rho(x,t) = 4 - 2\sec h^2(x - t)$$

The initial conditions are obtained from above equations by letting t = 0. We employed 901 grid points with domain $-30 \le x \le 30$, and free boundary condition at two ends. The results were output after 6000 time iterations as time marched to 20. The results are depicted in Figure 3. We compare the results of 1st order Roe's scheme (Roe1) and 2nd order WENO scheme (WENO2) with the exact solutions. Again, it can be easily seen the effect of higher order method and the proper working of the present methods. Our solution compares very well with that in [17].

The third test case is a quantum hydrodynamic shock tube flow initially with $\rho = 4 (x \le 0.)$, $\rho = 1 (x > 0)$ and $\nabla S = 0$ on both sides. Computational domain: $-0.5 \le x \le 0.5$. With 101 grid points, at time t = 0.1, the computational results using first order upwind, second-order ENO scheme, second and third order WENO schemes are shown in Figure 4. The high order methods give more crisp shock profile compared with the first order upwind method.

(ii) RBF scheme

To illustrate the practical applications of MQ method, the NLS and QFD equations are applied to simulate the following problems separately: (i) 1D BEC under standing light wave potential [4](ii) 2D BEC under standing light wave potential [5] (iii) 1D attractive BEC [1] (iv) 2D superfluid flow over a cylinder [25].There exist some adjustable parameters in MQ method such as shape factor c and the number of extended layers E, so we decide them by comparing existing analytical solutions of case (i) and (ii).

The first case is 1D BEC under an external standing light wave potential, the dimensionless 1D GP equation:

$$i\frac{\partial \psi(x,t)}{\partial t} = -\frac{1}{2}\frac{\partial^2 \psi(x,t)}{\partial x^2} + V(x)\psi(x,t) + |\psi(x,t)|^2 \psi(x,t)$$

$$V(x) = V_0 \sin^2(kx), V_0 = -1, k = 1$$

The initial conditions are

$$\psi(x,0) = \sqrt{B - \frac{V_0}{\alpha\beta(k)}\sin^2(kx)}\exp\{i\theta(x)\},$$

$$\tan[\theta(x)] = \sqrt{1 - \frac{V_0}{\alpha B\beta(k)}}\tan(kx) \qquad \alpha = 1, \beta = 1, B = 1$$

The results are shown in Figure 5.

The second case is 2D BEC under an external standing light wave potential,the dimensionless 2D GP equation:

$$i\frac{\partial \psi(x,y,t)}{\partial t} = -\frac{1}{2}\frac{\partial^2 \psi(x,y,t)}{\partial x^2} - \frac{1}{2}\frac{\partial^2 \psi(x,y,t)}{\partial y^2}$$

$$+V(x,y)\psi(x,y,t) + |\psi(x,y,t)|^2 \psi(x,y,t)$$

The results are shown in Figure 6.

The third case is the 1D focusing BEC free motion, the dimensionless 1D GP equation:

$$i\frac{\partial\psi}{\partial t}+\frac{\partial^2\psi}{\partial x^2}+2|\psi|^2\psi=0$$

The results are shown in Figure 7.

The forth case is 2D superfluid flow over a cylinder, the dimensionless 2D GP equation:

$$i\frac{\partial\psi(x,y,t)}{\partial t}=-\frac{1}{2}\frac{\partial^2\psi(x,y,t)}{\partial x^2}-\frac{1}{2}\frac{\partial^2\psi(x,y,t)}{\partial y^2}+\left(|\psi(x,y,t)|^2-1\right)\psi(x,y,t)$$

In this case, we used moving frame, GP equation becomes

$$i\frac{\partial\psi(x',y',t)}{\partial t}=-\frac{1}{2}\frac{\partial^2\psi(x',y',t)}{\partial x'^2}-\frac{1}{2}\frac{\partial^2\psi(x',y',t)}{\partial y'^2}+\left(|\psi(x',y',t)|^2-1\right)\psi(x',y',t)+i\vec{U}\cdot\left(\frac{\partial\psi(x',y',t)}{\partial x'}\hat{e}_i+\frac{\partial\psi(x',y',t)}{\partial y'}\hat{e}_j\right)$$

in the moving frame coordinates $\vec{r}'=x'\hat{e}_i+y'\hat{e}_j=\vec{r}-\vec{U}t$

The results are shown in Figure 8 and Figure 9 with velocity U=0.5.

Conclusion

Based on the present although preliminary, however, encouranging results for the quantum fluid dynamics, it is fair to conclude that the present method may provide an robust solution method to the nonlinear Schrödinger equations. The real challenge will be in the multi-dimensional problems with finite bounday conditions [21]. Progress towards this goal is currently underway and will be reported in a sequel.

The MQ scheme has been extended in this work to solve the NLS and QFD equations for Bose-Einstein condensations. 1D and 2D BEC with an external standing light wave potential can get accurate result using both NLS and QFD equations. However, when the solutions appear ”quantum vortex”, some problems appear in QFD equations, singular values appear in the computation, blow up solutions are caused by these singular values. Numerical method base on QFD equations has some numerical advantages, but its topological defects cause blow up problems in certain cases.

Acknowledgement

This work was supported by the National Science Council, Taiwan through grant NSC-93-2212-E-002-040.

References

1. A.L. Islas, C.M. Schober, FGCS, 19, 403-413.
2. A. L. Islas, D.A. Karpeev and C.M. Schober, J. Comput. Phys., 173, 116-148 (2001)
3. A. S. M. Wong, Y. C. Hon, T. S. Li, S. L. Chung, and E. J. Kansa, Comput. Math. Appli., 37 , 23-43, 1999.
4. B. Deconinck, J. N. Kutz, Phys. Lett. A,319,97, 2003.
5. B. Deconinck, B.A. Frigyik and J.N. Kutz, Phys. Lett. A, 283, 177, 2001.
6. B. Fornberg, T.A. Driscoll,G. Wright, and R. Charles,Comput.Math.Appl.,43,473-490,2002
7. C. Huepe, M. E. Brachet, Physica D, 140, 126-140, 2000.
8. B. K. Kendrick, J. Chem. Phys., 119, 5805-5817, 2003
9. C.J. Trahan and R.E. Wyatt, J. Comput. Phys., 185, 27-49 , 2003.
10. C. Nore, M. E. Brachet and S. Fauve, Physica D, 65, 154-162, 1993.
11. C. Sulem, P. L. Sulem, Springer, 1999.
12. G.S. Jiang and C.W. Shu, J. Comput. Phys., 126, 202-228, 1996.
13. J. C. Bronski, L. D. Carr, B. Deconinck, and J. N. Kutz, Phys. Rev. Letters, 86, 2001.
14. J. Y. Yang and C.A. Hsu, AIAA J., 30, 1570-1575 (1992)
15. J. Y. Yang, J. C. Huang and T. Y. Hsieh, ICCFD3,Toronto, Canada, July 12-16, 2004.
16. J. Y. Yang, Y. C. Perng and R. H. Yen, AIAA J., Vol.39, 2082-2090, 2001.
17. L. D. Carr, C. W. Clark, and W. P. Reinhardt, Physical Review A, Vol.62, 063610, 2000.
18. M. Adid, C. Huepe, S. Metens, C. Nore, C. T. Pham, L. S. Tuckerman, and M. E. Brachet, Fluid Dynamics Research,33,509-544, 2003.
19. M. Stone, A. M. Srivastava, J. Low Temp. Phys.,102,445-459,1996.
20. N.G. Berloff, P.H. Roberts, J. Phys. A:Math. Gen., 34, 81-89,2001
21. P.H. Roberts and R.J. Donnelly, Annu. Rev. Fluid Mech., 6, 1974.
22. P.R. Holland, Cambridge University Press, New York, 1993.
23. R. E. Wyatt and E.R. Bittner, Computing in Sci & Engi., 22, 2003.
24. R. J. Donnelly, Cambridge University Press, Cambridge, 1991.
25. T. Frisch, Y. Pomeau, and S. Rica, Phys. Rev. Lett., 69, 1644-1647, 1992.
26. T.Winieck, J.F.McCann, and C.S. Adams, Phys. Rev. Lett., 82, 5186-5189, 1999.
27. T. Y. Hsieh, J. C. Huang and J.Y. Yang, ICCFD3,Toronto, Canada, July 12-16, 2004.
28. W. Bao, D. Jaksch, P. A. Markowich, J. Comput. Phys., 187, 318-342, 2003.
29. W. Bao, S. Jin and P. A. Markowich, SIAM J. Sci. Comput., 2003.
30. W. H. Raymond, H. L. Kuo, Quart. J. R. Met. Soc., 110, 535-551, 1984.
31. X.G. Hu, T.S. Ho and H. Rabitz, Comput. Math. Appl., 43, 525-537, 2002.
32. Y.C. Hon, K.F. Cheung, X.Z. Mao and E.J. Kansa, J. Hydr. Engrg., 125,524-533, 1999.

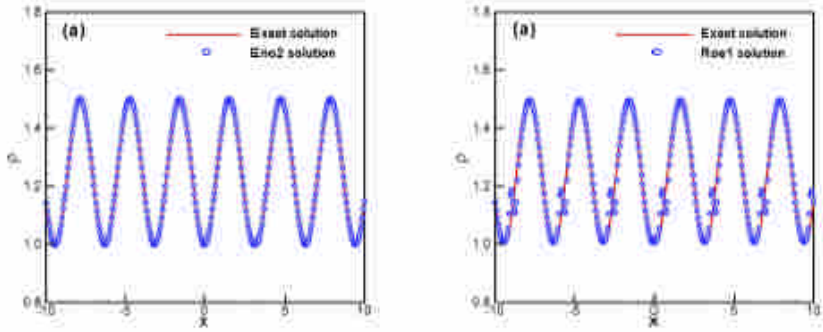

Fig. 1. Solution of test case 1: $\rho = |\psi|^2$. (a)Roe1, (b)ENO2.

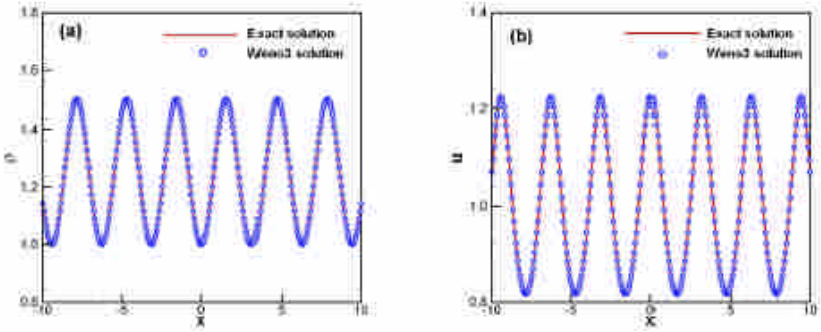

Fig. 2. Solution of test case 1 by 3rd order WENO scheme. (a)$\rho = |\psi|^2$, (b) $u = \nabla S$

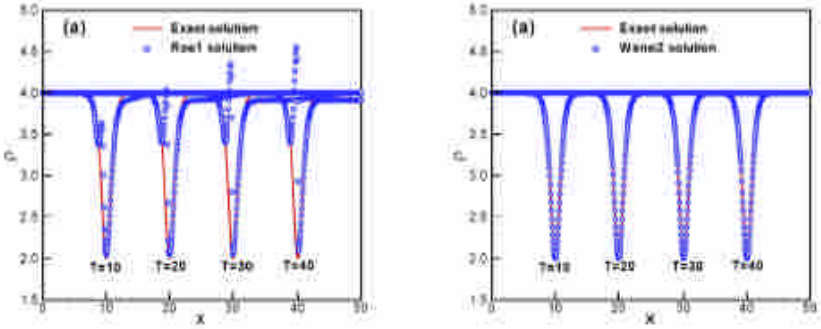

Fig. 3. Solution of test case 2: $\rho = |\psi|^2$. (a)Roe1, (b)WENO2.

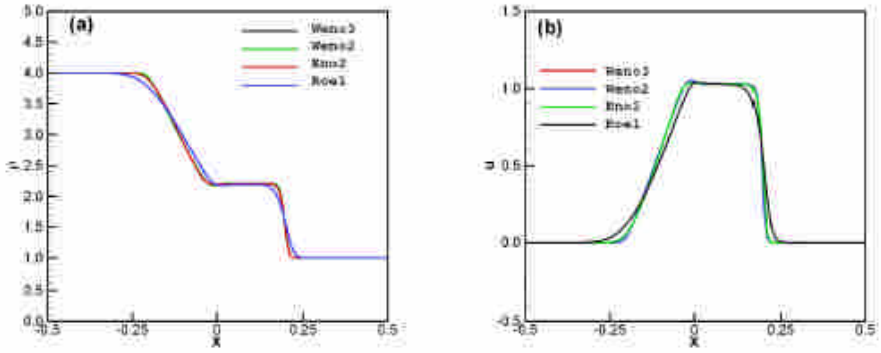

Fig. 4. A comparison of solutions for quantum shock tube flow. (a)$\rho = |\psi|^2$,(b) $u = \nabla S$

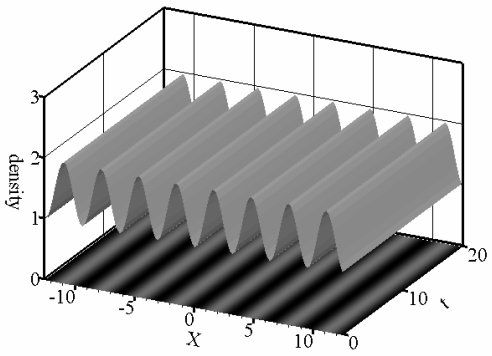

Fig. 5. Long time solution of density.

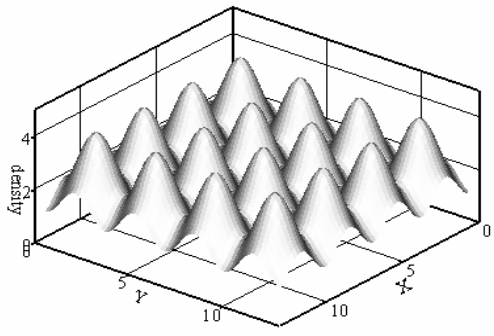

Fig. 6. Density at time t=20.

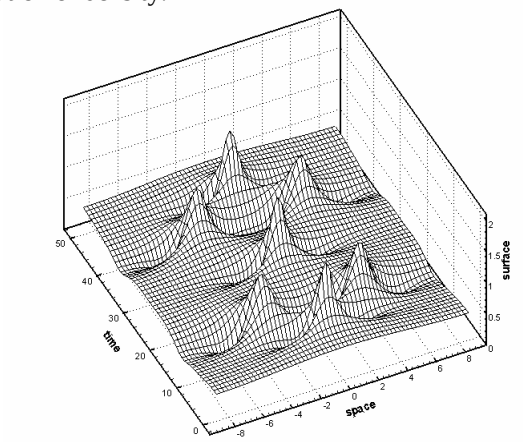

Fig. 7. Long time solution of surface |ψ|.

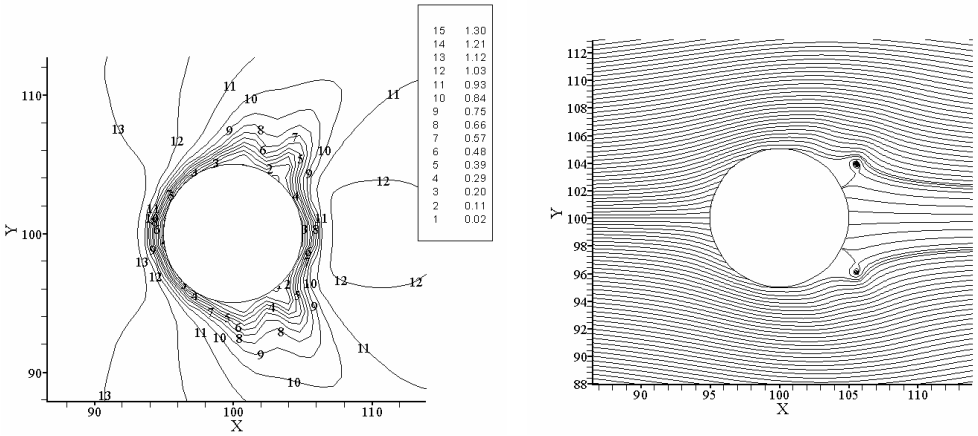

Fig. 8. Density and streamline at t=20.

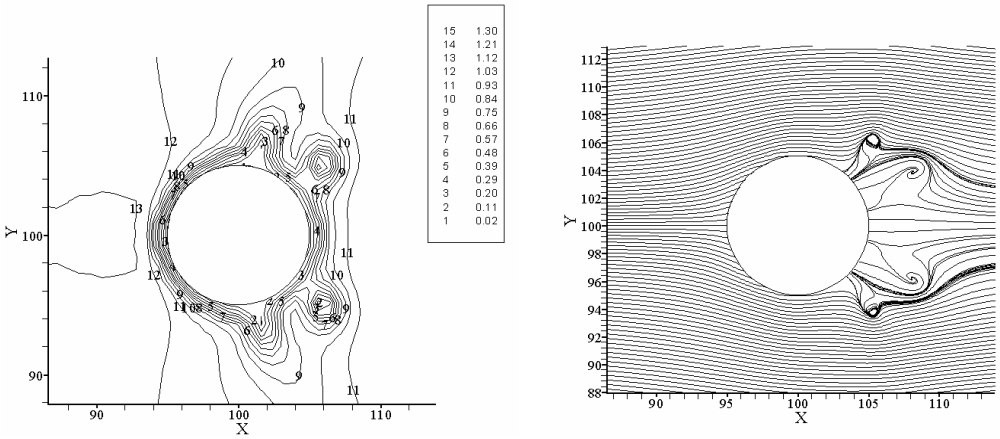

Fig. 9. Density and streamline at t=30.